

# Cell Cycle of Myocytes of Cardiac and Skeletal Muscle in Mitochondrial Myopathy

Atsushi Takeda, MD; Satoru Chiba, MD\*; Iwai Takaaki, MD; Akira Tanamura, MD;  
Yutaka Yamaguchi, MD\*; Nobuakira Takeda, MD

Patients who have mitochondrial myopathy can present with specific pathological conditions (eg, diabetes mellitus and deafness). A 36-year-old woman presented with mitochondrial myopathy, encephalopathy, lactic acidosis and stroke-like episodes (MELAS). An investigation was conducted into whether the abnormality of mitochondrial DNA (a T to C transition at position 3271 in the mitochondrial tRNA [*Leu(UUR)*] gene) influences nuclear DNA synthesis by cells in the heart, skeletal muscles, and brain. Myocardium, skeletal muscle, and brain tissues were stained with hematoxylin-eosin, and Masson trichrome for histopathology. Target nuclei taken from the myocardial and skeletal muscles and brain tissue were purified after removing debris by the modified Hedley method. These nuclei were stained with propidium iodide (PI) for analysis by flow cytometry. The number of nuclei in the G2M phase was bigger in myocytes of MELAS than in normal myocytes (Control) (MELAS myocyte: Control myocyte=24.9±7.3: 6.1±1.6%,  $p<0.005$ ), but there was no significant increase in the G2M phase in brain tissue. The G1 phase was far more reduced in MELAS myocytes and skeletal muscle than in Controls (MELAS myocyte: Control myocyte=65.8±9.1: 88.0±3.2%,  $p<0.005$ ; MELAS skeletal muscle: Control skeletal muscle=85.1±2.2: 90.1±3.2%,  $p<0.05$ ), while there was no significant decrease of nuclei in the G1 phase in brain tissue. Increased amount of nuclei in the G2M phase in cardiac myocytes and skeletal muscle cells compared with that in neurons might depend on the capacity for proliferation and differentiation of these cells as compared with brain tissue. It was concluded that the mitochondrial DNA mutation (3271T-to-C) of MELAS may influence the nuclear DNA synthesis of cells in various tissues depending on their level of mitotic activity. (Jpn Circ J 1998; **62**: 695–699)

**Key Words:** Cell cycle; DNA; Gene; Mitochondria; Myopathy

Mitochondrial DNA (mtDNA) is located in the matrix and is sometimes found attached to the inner mitochondrial membrane. Human mtDNA is a completely sequenced circular structure of 16,569 bp. Human mtDNA encodes 2 rRNAs and 22 tRNAs. Normal and abnormal mitochondrial DNA co-exist in mammalian cells, which is called 'heteroplasmy', and the ratio of the 2 types of mtDNA differs among tissues.<sup>1–3</sup> Therefore, patients who have mtDNA mutations may present with various symptoms and diseases; for example, mitochondrial myopathy (MELAS)<sup>4,5</sup> diabetes mellitus,<sup>6,7</sup> cardiomyopathy<sup>4</sup> deafness<sup>6</sup> and others.<sup>8</sup>

Several recent reports on MELAS have suggested that mutations of mtDNA, especially substitution of A to G at position 3243 of the leucine tRNA (3243 mutation), may cause diabetes and deafness.<sup>9–11</sup> The 3243 point mutation has been recognized in about 1–2% of patients with diabetes mellitus.<sup>10,12–14</sup>

We report here on a 36-year-old woman who was finally diagnosed as MELAS because she had epilepsy, lactic acidosis, an mtDNA 3271 point mutation (a T to C transition at position 3271 in the mtDNA), and ragged-red fibers

in biopsy material of skeletal muscle. We investigated whether this mtDNA point mutation influenced cell proliferation in several organs (heart, skeletal muscle, and brain). Nuclear DNA synthesis in cardiac myocytes, skeletal muscle cells, and brain tissue was investigated by flow cytometry analysis.

## Case Report

### Patient Profile

The patient was a 36-year-old housewife with the chief complaint of headache. There was nothing specific in her past medical or family history.

**Present Illness:** She visited the Neurosurgery Department of our hospital because of the headache on October 1, 1994. Her neurological findings and brain computed tomography (CT) scan were almost normal on that same day, although she had sustained headache with muscle cramps. 1 week later, she was hospitalized because of disturbed consciousness, syncope, and left hemiparesis. The diagnosis was cerebral infarction.

**Physical Findings:** Her height was 145 cm, body weight was 31 kg, consciousness was drowsy, blood pressure was 110/60 mmHg, and heart rate was 100 beats/min (regular). There was left hemiparesis and muscle cramping.

**Laboratory Data:** The blood lactate level was 47.5 mg/dl (normal: 1–27 mg/dl) and the pyruvic acid level was 2.13 mg/dl (normal: <1.02 mg/dl). ECG showed sinus tachycardia (Fig 1). Brain CT showed multiple low density areas in the cerebrum.

(Received December 8, 1997; revised manuscript received April 20, 1998; accepted April 27, 1998)

Department of Internal Medicine, Aoto Hospital, and \*Department of Pathology, Kashiwa Hospital, Jikei University School of Medicine, Tokyo, Japan

Mailing address: Atsushi Takeda, MD, Department of Internal Medicine, Aoto Hospital, Jikei University School of Medicine, Aoto 6-41-2, Katsushika-Ku, Tokyo 125, Japan

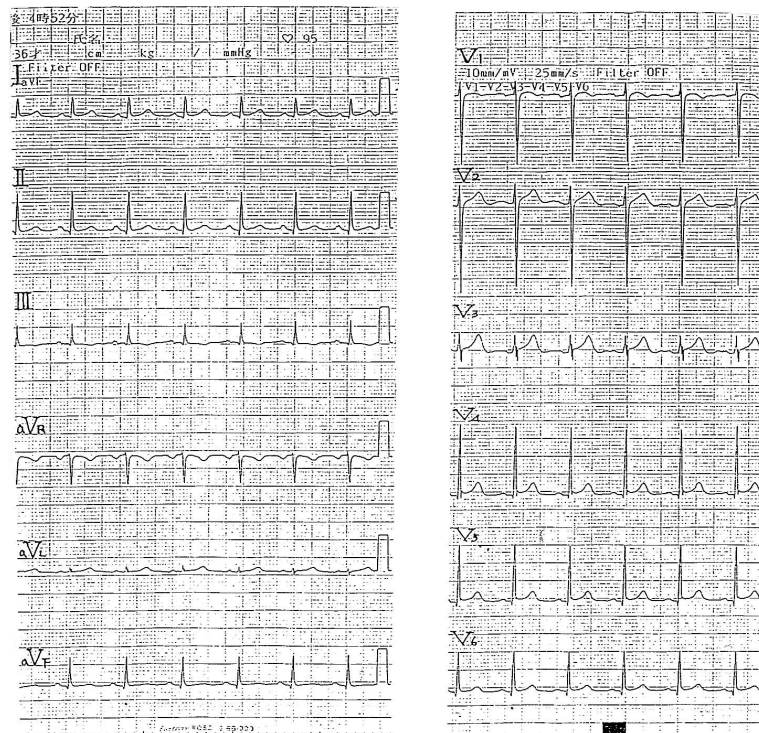


Fig 1. Electrocardiogram of the 36-year-old MELAS patient.

Masson trichrome staining of the skeletal muscle biopsy taken for the MELAS diagnosis revealed ragged-red fibers and hypertrophic and atrophic muscle fibers (Fig 2).

**Mitochondrial DNA Analysis:** A mtDNA (3271) point mutation was identified in the skeletal muscle mitochondria obtained from the biopsy specimen.

**Progress after Admission:** She was treated with steroids and glycerol after diffuse patchy cerebral infarctions were found on October 8, but her cramping and disorientation persisted. The low density areas on brain CT showed a skip lesion compared with the previous findings, so the patient was diagnosed as MELAS syndrome based on the mtDNA analysis, skeletal muscle biopsy, and biochemical data. She was then treated with coenzyme Q<sub>10</sub>, but died of MRSA infection on June 6, 1995.

#### Materials and Methods

At autopsy, heart muscle, skeletal muscle, and brain tissue were obtained for analysis. Several pieces of tissue were cut from each organ for flow cytometry analysis of the cell cycle.

**Pathological Study:** Myocardium, skeletal muscle, and brain tissue were stained with hematoxylin-eosin and Masson trichrome after routine 10% formalin fixation, paraffin embedding and sectioning. These tissues were also examined by transmission electron microscopy.

**Cell Cycle Analysis with Flow Cytometry:** The percentage ratios of each phase were calculated automatically with the integral calculus by FACS flow cytometry (Becton Dickinson Co)<sup>15-17</sup> With 4 different samples from each organ (heart, skeletal muscle, brain tissue), the cell cycles were measured by flow cytometry, and statistical analyzes were performed comparing each with normal controls (heart, skeletal muscle, brain tissue). Several 60-μm sections were cut from each paraffin block of tissue<sup>18</sup> and placed in tubes with xylene for 20 min and then gradually

rehydrated with distilled water. The sample tubes were then incubated for 1 h at 37°C in a water bath after adding 1 ml of 0.5% pepsin solution (pH 1.5) in 0.9% NaCl. After pipetting off this solution, target nuclei were purified by filtering through a 30–60 μm teflon mesh to remove debris (modified Hedley method)<sup>19,20</sup> The nuclei were then stained with 50 μg/ml propidium iodide (PI) and 0.1% Triton X-100 in 4 mmol/l sodium citrate (Vindelov method). This solution was centrifuged (4°C, 400 × g, 10 min), the supernatant was discarded, 0.5 ml of PI solution was added, and then a FACSscan (Becton Dickinson Co) was used for flow cytometry<sup>15,16,21,22</sup>

In the fluorescein DNA histogram, the first high peak indicated the G0–1 phase of cell cycle, and also the second peak is the G2M phase. The valley between the G0–1 and G2M phases shows the S phase<sup>15,16</sup> (Fig 7). The DNA frequency histogram was deconvoluted and the results were computer analyzed using the Multicycle software (Phoenix Flow System, San Diego, CA, USA)<sup>15,16</sup> Results are presented as mean ± SD. Comparisons between the values of MELAS and Controls were performed using Student's t-test. A p value of less than 0.05 was considered statistically significant.

## Results

#### Histopathological Study

In the myocardial tissue, myocardial degeneration and perinuclear vacuolization of the cells were observed. The fine perinuclear granules of the myocyte seen by light microscopy could be seen to be mitochondria with the electron microscope (Fig 3). A variety of mitochondrial shapes and mitochondrial proliferation could be also observed in the myocardium (Figs 4,5). Myofibrilysis of skeletal muscle cells was also detected and perinuclear fine granules were observed in the cytoplasm.

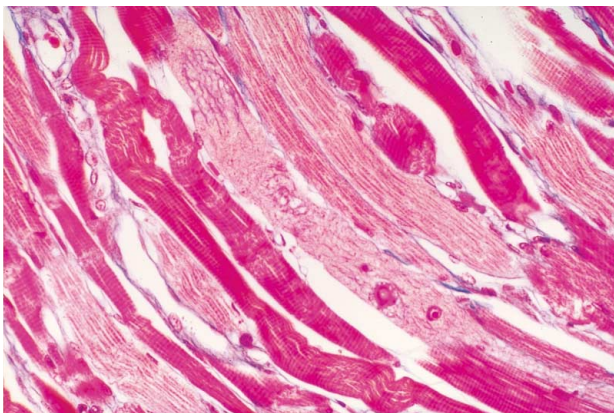


Fig 2. Skeletal muscle biopsy from the MELAS patient (Masson trichrome stain,  $\times 400$ ).

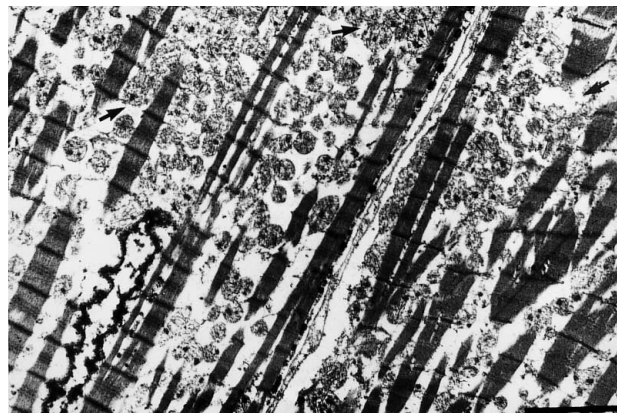


Fig 5. Left ventricular myocardial tissue from the MELAS patient (Masson trichrome stain,  $\times 400$ ).

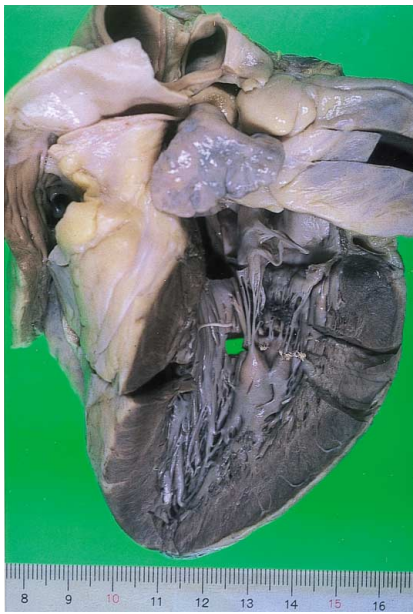


Fig 3. Transmission electron microscopy of the left ventricular free wall. Bar =  $5\text{ }\mu\text{m}$ .

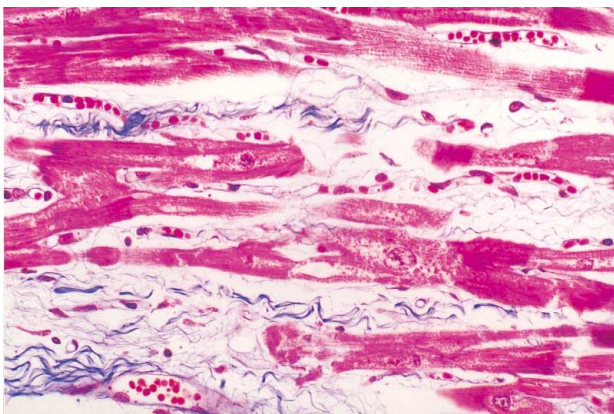


Fig 4. Macroscopic view of the heart from the MELAS patient.

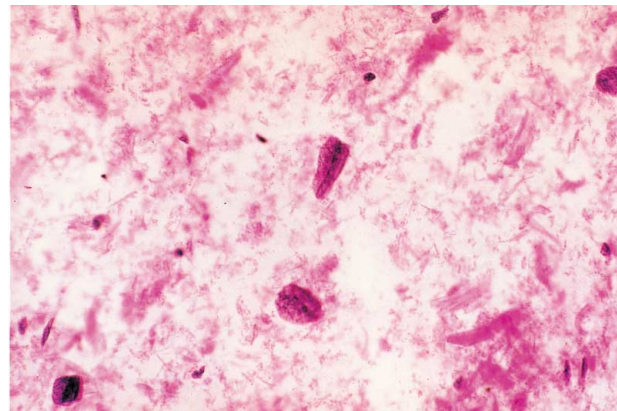


Fig 6. The naked nucleus after nuclear DNA analysis with hematoxylin-eosin stain ( $\times 600$ ).

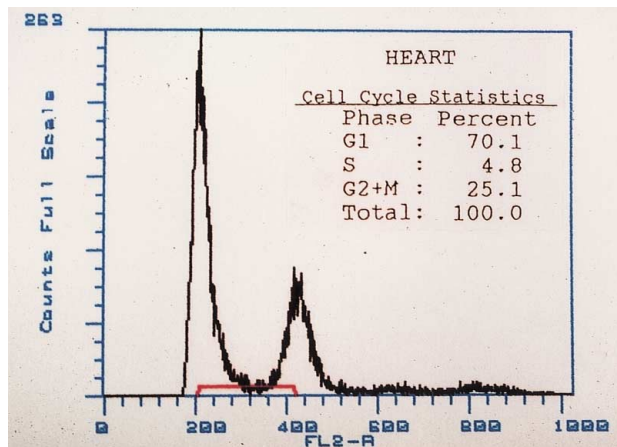


Fig 7. The fluorescein DNA histogram of a myocyte; the first high peak is the G0-1 phase and the second one is the G2M phase.

myocyte: Control myocyte= $24.9 \pm 7.3$ :  $6.1 \pm 1.6\%$ ,  $p < 0.005$ ; MELAS skeletal muscle: Control skeletal muscle= $6.4 \pm 1.0$ :  $4.7 \pm 1.8$ ,  $p < 0.005$ ), but there was no significant increase of the G2 phase in brain tissue. The extent of the G1 phase was significantly less in MELAS myocytes and skeletal muscles than in controls (MELAS myocyte: Control myocyte= $65.8 \pm 9.1$ :  $88.0 \pm 3.2\%$ ,  $p < 0.005$ ; MELAS skeletal muscle: Control skeletal muscle= $85.1 \pm 2.2$ :  $90.0 \pm 3.2\%$ ,

**Table 1 Cell Cycle of Neurons and Cardiac and Skeletal Muscle Cells**

	Cardiac muscle	Skeletal muscle	Brain tissue
G1 phase (%)	65.8±9.1** (88.0±3.2)	85.1±2.2* (90.0±3.2)	90.8±1.5 (93.0±2.6)
S phase (%)	8.3±3.1 (6.0±1.8)	8.5±2.9 (5.2±1.4)	7.4±2.4 (5.4±2.2)
G2M phase (%)	24.9±7.3** (6.1±1.6)	6.4±1.0** (4.7±1.8)	1.8±0.9 (1.7±1.5)

n=4, mean ± SD. \*p<0.05, \*\*p<0.005, vs Control (Control data).

p<0.05), but there was no significant difference in the G1 phase of brain tissue (Table 1).

With regard to the selection of nuclei, the average nuclear size in the myocardium was measured in hematoxylin-eosin stained tissue using the light microscope. Only myocardial nuclei were filtrated through the optimum Teflon mesh, whose hole size was a little bit smaller than size of the nuclear myocyte, and then almost all the nuclei of the interstitial cells were taken out (Fig 6). However, the mixing ratio (%) of interstitial cell nuclei was technically between about 2 and 8% (somewhere round 6%) after the measurement.

## Discussion

In mammals, cell differentiation and regeneration is continuous. The varying lifespans of cells are dependent on their ability to undergo mitosis modified by cell differentiation and regeneration.

Generally, mammalian cells are classified into 3 different mitotic categories: (i) vegetative intermitotics; (ii) reverting postmitotics; and (iii) fixed postmitotics.

As reverting postmitotics, hepatocytes, secretory gland cells, and renal tubular cells can undergo mitosis for regeneration after tissue damage. In other words, these cells are normally postmitotic, but proliferative activity can be reactivated to allow regeneration.

On the other hand, fixed postmitotic cells like neurons appear to lose the ability to regenerate and proliferate. Thus, the various kinds of cells show different levels of differentiation and regeneration. Our data suggested that skeletal muscle cells and cardiac myocytes were reverting postmitotic cells, whereas brain tissue cells were fixed postmitotic cells. This is supported by the finding that the G2M phase was lower in neurons than in the other cells. In the case of skeletal muscle, each cell has many nuclei, unlike other kinds of cells, so the amount of stimulation per nucleus may be reduced and the cell cycle may not progress to the G2 phase. In the present study, all the filtered nuclei were not from myocytes, with about 6% from interstitial cells. So the levels of the S and G2M phases obtained must be a little higher than is the case when all the nuclei are from myocytes. However, this influence is so little as to be somewhat ignored.

In conclusion, the difference in the extent of the G2M phase between cardiac myocytes or skeletal muscle cells and neurons might depend on the cell's capability of proliferating and differentiating. Also the difference between cardiac myocytes and skeletal muscle cells (myocytes: skeletal muscle cells=24.9±7.3: 6.4±1.0%) may depend on the severity of damage and the level of adaptation of the cells. About 25% of cardiac myocytes were in the G2 phase in MELAS syndrome.

We could not observe microscopically any double nuclear myocytes in the heart tissue from the MELAS patient and there were few polyploid cells by flow cytometric analysis, unlike in hypertrophic cardiomyopathy, dilated cardiomyopathy and hypertensive heart disease.

## Acknowledgments

The authors would like to thank Dr Yutaka Yamaguchi (Department of Pathology, Kashiwa Hospital, Jikei University School of Medicine) for providing the samples of MELAS syndrome.

This study was partly supported by the Research Committee for Epidemiology and Etiology of Idiopathic Cardiomyopathy of the Ministry of Health and Welfare of Japan, and a research grant from the Vehicle Racing Commemorative Foundation.

## References

- Eckenrode VK, Levings CS: In vitro review, Maize mitochondrial genes. *In Vitro Cell Dev Biol* 1986; **22**: 169–176
- Leving CS, Brown GG: Molecular biology of plant mitochondria (review). *Cell* 1989; **56**: 171–179
- Ozawa T, Katsumata K, Hayakawa M, Yoneda M, Tanaka M, Sugiyama S: Mitochondrial DNA mutation and survival rate. *Lancet* 1995; **345**: 189
- Ito T, Hattori K, Obayashi T, Tanaka M, Sugiyama S, Ozawa T: Mitochondrial DNA mutations in cardiomyopathy. *Jpn Circ J* 1992; **56**: 1045–1053
- Goto Y, Nonaka I, Horai S: A new mtDNA mutation associated with mitochondrial myopathy, encephalopathy, lactic acidosis and stroke-like episodes (MELAS). *Biochim Biophys Acta* 1991; **1097**: 238–240
- Remes AM, Majamaa K, Herva R, Hassinen IE: Adult onset diabetes mellitus and neurosensory hearing loss in maternal relatives of MELAS patients in a family with the tRNA Leu (UUR) mutation. *Neurology* 1993; **43**: 1015–1020
- Ohnishi H, Inoue K, Osaka H, Kimura S, Nagamoto H, Hanihara T, et al: Mitochondrial myopathy, encephalopathy, lactic acidosis and stroke-like episodes (MELAS) and diabetes mellitus, molecular genetic analysis and family study. *J Neurol Sci* 1993; **114**: 205–208
- Johns DR: Mitochondrial DNA and disease. *N Engl J Med* 1995; **333**: 638–644
- Kobayashi Y, Momoi YM, Tomiyama T, Momoi K, Nihei M, Yanagisawa M, et al: A point mutation in the mitochondrial tRNA Leu (UUR) gene in MELAS (mitochondrial myopathy, encephalopathy, lactic acidosis and stroke-like episode). *Biochem Biophys Res Commun* 1990; **173**: 816–822
- Goto Y, Nonaka I, Hori S: A mutation in the tRNA Leu (UUR) gene associated with the MELAS subgroup in mitochondrial encephalomyopathies. *Nature* 1990; **348**: 635–651
- Ouwendijk JMW, Lemkes H.P.J., Maassen JA: Mutation in mitochondrial tRNA Leu (UUR) gene in a large pedigree with maternally transmitted type II diabetes mellitus and deafness. *Nature Genet* 1992; **1**: 368–371
- Kadowaki T, Kadowaki H, Mori Y, Tabe K, Sakuta R, Suzuki Y, et al: A subtype of diabetes mellitus associated with a mutation of mitochondrial DNA. *N Engl J Med* 1994; **330**: 962–968
- Oka Y, Katagiri H, Yazaki Y, Murase T, Kobayashi T: Mitochondrial gene mutation in islet-cell-antibody-positive patients who were initially non-insulin-dependent diabetics. *Lancet* 1993; **342**: 527–528
- Reardon W, Ross RJM, Sweeney MG, Luxon LM, Pembrey ME, Harding AE, Trembath RC: Diabetes mellitus associated with a pathogenic point mutation in mitochondrial DNA. *Lancet* 1992; **340**: 1376–1379
- Fried J: Method for the quantitative evaluation of data from microfluorometry. *Comput Biomed Res* 1976; **9**: 263
- Dean PN, Jett JH: Mathematical analysis of DNA distributions derived from flow microfluorometry. *J Cell Biol* 1974; **60**: 523
- Baba HA, Takeda A, Schmid C, Nagano M: Early proliferative changes in hearts of hypertensive Goldblatt ratio: an immunohistochemical and flow-cytometrical study. *Basic Res Cardiol* 1996; **91**: 275–282
- Stephenson RA, Gay H, Fair WR: Effect of section thickness on quality of flowcytometric DNA content determinations in paraffin-embedded tissue. *Cytometry* 1986; **7**: 41–44
- Hedley DW, Friedlander ML, Taylor IW: Method for analysis of cellular DNA content of paraffin-embedded pathological materials

using flow cytometry. *J Histochem Cytochem* 1983; **31**: 1333–1335

20. Hedley DW, Friedlander ML, Taylor IW: Application of DNA flow cytometry to paraffin-embedded archival material for the study of aneuploid and clinical significance. *Cytometry* 1985; **6**: 327–333

21. Reynder SB, Bosman MJ: Flow cytometric determination of DNA ploidy level in nuclei isolated from paraffin-embedded tissue. *Cytometry* 1985; **6**: 26–30

22. Vindelov LL, Christensen IJ, Nissen NI: A detergent-trypsin method for the preparation of nuclei for flow-cytometric DNA analysis. *Cytometry* 1983; **3**: 323–327